Stick-slip fluctuations in granular drag

I. Albert,[1] P. Tegzes,[1,2] R. Albert,[1] J. G. Sample,[1] A. -L. Barabási,[1] T. Vicsek,[2] B. Kahng,[3] and P. Schiffer[1,4,*]

[1]*Department of Physics, University of Notre Dame, Notre Dame, Indiana 46556*
[2]*Department of Biological Physics, Eötvös University, Budapest 1117, Hungary*
[3]*Center for Theoretical Physics and School of Physics, Seoul National University, Seoul 151-742, Korea*
[4]*Department of Physics and Materials Research Institute, Pennsylvania State University, University Park, Pennsylvania 16802*

We study fluctuations in the drag force experienced by an object moving through a granular medium. The successive formation and collapse of jammed states give a stick-slip nature to the fluctuations which are periodic at small depths but become "stepped" at large depths, a transition that we interpret as a consequence of the long-range nature of the force chains and the finite size of our experiment. Another important finding is that the mean force and the fluctuations appear to be independent of the properties of the contact surface between the grains and the dragged object. These results imply that the drag force originates in the bulk properties of the granular sample.

I. INTRODUCTION

The propagation of stress in granular media presents a complex problem which has been the subject of extensive study [1]. An applied external stress results in the development of an internal structure resisting the stress, a so-called jammed state that is dependent on the direction and magnitude of the stress [2]. The origins of this jamming lie in the fact that the forces do not propagate uniformly through the granular sample but are localized along directional force chains [3–10], and the jammed state is ultimately characterized by the properties of the network of these chains.

In this paper we investigate the jamming of spherical granular media by analyzing the drag force opposing the movement of a solid object through such media. The object's motion is opposed by jamming of the grains in front of the object, but if the applied force exceeds a critical threshold corresponding to the strength of the jammed state, the object moves ahead while displacing the surrounding grains. Such successive breakdowns result in large fluctuations in the drag force at low velocities, which reflect the strength of successive jammed states. Our results demonstrate that the forces arising from such jamming of the grains and subsequent bulk grain reorganization dominate the drag process while the frictional forces at the surface have little effect. Furthermore, the nature of the fluctuations, and thus the strength of the jammed states, can be affected by the finite size of the containing vessel due to the long-range nature of the force chains. Some of the results have been published previously [11].

II. DESCRIPTION OF THE APPARATUS

The experimental apparatus, shown in Fig. 1, consists of a vertical steel cylinder of diameter d_c inserted to a depth H in a cylindrical container filled with glass spheres. A comb made of three 5 mm diameter steel rods separated by 20 mm

gaps is also inserted at 150 mm depth opposite the vertical cylinder with the role of randomizing the medium. This comb has the additional benefit of stabilizing the packing fraction during the experimental runs.

The container rotates with constant angular speed while the vertical cylinder is attached to an arm that may rotate freely around the rotational axis of the container. Opposing the cylinder we have a fixed precision force cell [12] which measures the force $F(t)$ acting on the cylinder as a function of time. We also incorporate a spring of known spring constant k between the cylinder and the force cell with k varying between 5 and 100 N/cm. The purpose of the spring is twofold; it allows the force to slowly build up, and with a suitable choice of k it dominates the elastic response of the cylinder and all other parts of the apparatus so that the nonlinear deformations will not significantly affect the results. We vary the speed (v) from 0.04 to 1.4 mm/s, the depth of insertion (H) from 20 to 190 mm, and the cylinder diameter (d_c) from 8 to 24 mm, studying glass ($\rho = 2.5$ g/cm^3) spheres of diameter (d_g) 0.3, 0.5, 0.7, 0.9, 1.1, 1.4, 1.6, 3.0, and 5.0 mm. The force is sampled at 150 Hz and the response times of the force cell and the amplifier are less than 0.2 ms.

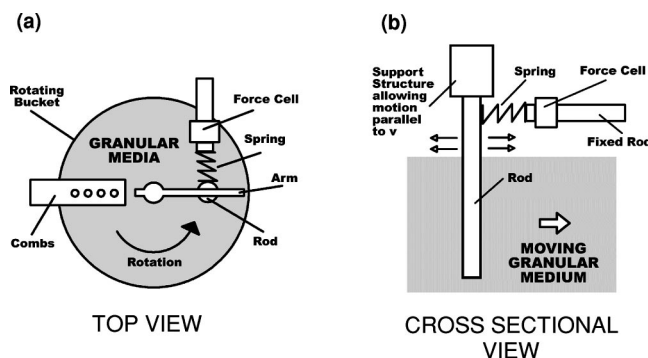As we will discuss in detail later, the drag force experi-

FIG. 1. Schematic view of the apparatus used for measuring the drag force. The grains were contained within a 25 cm diameter rotating bucket as described in detail previously [11]. (a) Top view; (b) cross-sectional view.

*Email address: schiffer@phys.psu.edu

enced by the vertical cylinder, $F(t)$, is not constant, but has large stick-slip fluctuations consisting of linear rises associated with a compression of the spring and sharp drops (sudden decompressions of the spring) corresponding to the collapse of the jammed grains opposing the motion. In most of our measurements the angular deflection of the arm during the fluctuations was around $1°$ ($\approx$ one bead diameter); therefore in subsequent discussions we have approximated the spatial deflection of the cylinder as linear. Note that these experiments are conducted in dense static granular media as opposed to drag in dilute or fluidized media which has been studied both theoretically [13] and experimentally [14]. In our experiments, however, all grains are at rest relative to each other and the container for the vast majority of the time.

During the stick process the cylinder is stationary relative to the granular medium moving with speed v. During this process the spring is compressed at a uniform rate. Thus the change in the force on the cylinder is described by $\Delta F = k\Delta x = kvt_{stick}$. The slip processes, during which the cylinder moves relative to the medium, are very short when compared to the duration of the stick processes $t_{slip} \ll t_{stick}$ for all depths. Although t_{stick} changes with depth (ΔF has H dependence) t_{slip} stays approximately the same, and it is comparable to the characteristic inertial time $\tau_{in} = 2\pi\sqrt{M/k} \approx 0.1$ s. As long as t_{stick} is significantly larger than t_{slip} the stick-slip process probes the properties of the material, but if k is chosen very large so that the quantity $t_{stick} = \Delta F/kv$ is comparable to τ_{in} the dynamics will be dominated by the inertial properties of the apparatus. Additionally, k must be chosen such that it is much smaller than the elasticity of the apparatus. These conditions impose certain limits for acceptable values of v and k in a somewhat similar way as with sliding surface friction [15]. As we will show later, however, within these limits the average force and fluctuations are not affected by the choice of either v or k.

III. DATA ANALYSIS

During each fluctuation the force first rises to a local maximum (the stick process) and then drops sharply as the jammed state collapses (the slip process). As shown in Fig. 2 we have identified three characteristic types of stick-slip motion. These three types, as explained in detail below, are as follows.

Periodic: The signal resembles an ideal sawtooth signal. The distributions of maxima and minima have narrow widths that do not overlap within two standard deviations. We observe this behavior for beads of diameter $d_g = 0.3, 0.5, 0.7, 0.9,$ and 1.1 mm and depths less than 100 mm.

Random: The signal resembles a random sawtooth signal. The distributions of maxima and minima overlap within one standard deviation. Only beads of diameter larger than 1.1 mm, $d_g = 1.4, 1.6, 3.0,$ and 5.0 mm, exhibit this behavior. We attribute the appearance of random fluctuations to the finite size effects associated with both the container size and the cylinder/bead ratio. Because of the complications introduced by these effects, in the present paper we focus on the other two regimes and we plan to study this random regime in more detail in another experiment.
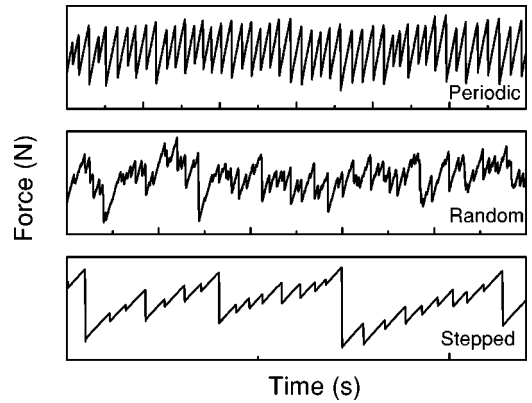

FIG. 2. Graphical representation of the drag force fluctuations in the three observed regimes, periodic, random, and stepped. Transitions between these regimes are determined by parameters like grain size, insertion depth, and cylinder diameter.

Stepped: The force builds up as a sum of small sawtooth-like steps. Each subsequent maximum and minimum tends to be at a higher force than the previous one, until a large reorganization occurs that resets the system and the incremental buildup starts again. This behavior can be observed at large depth ($H > 140$ mm), and the transition from the periodic to the stepped regime can be well characterized. As we will show later, the container diameter has an influence on the critical depth at which the periodic regime changes into the stepped one.

In each of these regimes the quantity $(1/v)dF/dt$ in the stick processes stays constant and equal to k, thus serving as strong evidence that during the stick processes the cylinder is at rest relative to the granular reference frame. We note that we did not observe precursors to the slip events even for the lowest speeds (0.05 mm/s) and weakest springs (5 N/m), cases that offered the best time resolution. We believe that the gradual, plastic yield observed right before slipping of two-dimensional sheared granular layers [18] does not take place in our system. We have extensively studied both the periodic regime and the transition from the periodic to the stepped regime.

A. The periodic regime

1. General characteristics

This regime has been observed for all beads with $d_g < 1.4$ mm and depths H smaller than 80 mm. A characteristic data set and power spectrum [the squared amplitudes of the Fourier components of $F(t)$] are shown in Fig. 3. As discussed below, the power spectra allow us to examine how the fluctuations scale with velocity and spring constant and also allow us to compare data taken with different cylinders.

As seen on the spectrum, the low frequency interval is dominated by the Fourier terms corresponding to the periodicity of the signal. We observe only one or two higher order harmonics, while at higher frequencies the spectra exhibit power law scaling with exponent of -2. Similar scaling was also observed in sheared granular materials in a Couette geometry [4], and is intrinsic to random sawtooth signals [16].
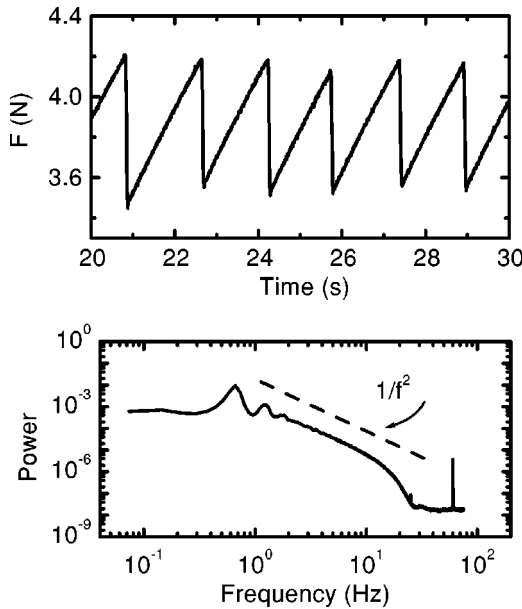
FIG. 3. The signal shape and the power spectrum in the periodic regime ($d_c=10$ mm, $d_g=0.9$ mm, and depth $H=80$ mm). The lower graph shows a typical power spectrum for this regime. The dashed line has the slope of -2.

At high frequencies we see only electronic noise.

In the periodic regime, the signal $F(t)$ is made up by continuous rises to a maximum value (F_{max}) followed by drops to a minimum (F_{min}). As shown on Fig. 4, the widths of the distributions for the maxima and minima are roughly the same and the histograms do not intersect. We may consider the separation between the mean values of maxima and minima as a parameter in distinguishing the periodic regime from the random one. This parameter has a purely statistical interpretation, 4σ separation meaning that $\approx 96\%$ of the minima were smaller than $\approx 96\%$ of the maxima. The size distribution of upward and downward jumps (the difference between the values of consecutive minima to maxima and maxima to minima) is quite similar, as shown in Fig. 5.

We observed no significant correlation between consecutive values of maxima and minima; thus we may consider
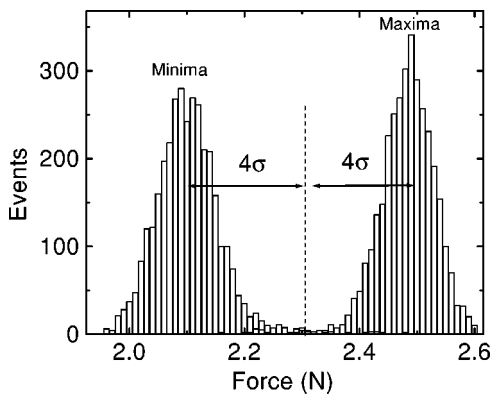

FIG. 4. Distribution of maxima and minima in the periodic regime. ($d_c=16$ mm, $d_g=0.9$ mm and $H=60$ mm.) The large separation between the peaks of the histograms for the maxima and minima characterizes the periodic regime.
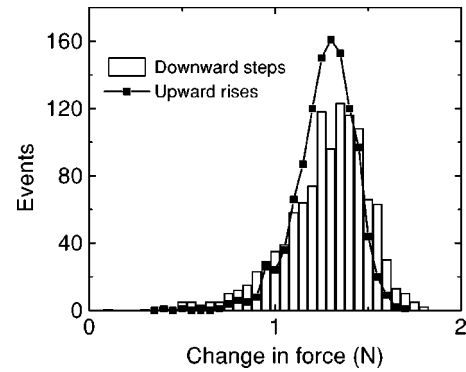

FIG. 5. Fluctuation (upward rise and downward step) distribution in the periodic regime for $d_c=16$ mm, $d_g=0.9$ mm, and $H=80$ mm. The upward rises correspond to height differences from a minimum to the next maximum. Downward steps correspond to changes from a maximum to the next minimum (absolute values).

them independent random variables. The interval-averaged values, computed as the average values of the maxima or minima over an interval (50 points), however, show a correlated overall modulation with an amplitude of about $\pm 5\%$ of the total value. Since this modulation affects both the maxima and the minima identically, it appears to be caused by small changes of the jamming properties of the medium in different parts of the container. Such changes might be caused by inhomogeneities in the packing or surface level associated with inserting and removing the cylinder.

2. Depth, cylinder diameter, and grain diameter dependence

In a previous paper [17] we reported that the drag force on a cylinder with diameter d_c inserted to a depth H in a granular bed can be written as $\bar{F}=\eta\rho g d_c H^2$ where η characterizes the grain properties (surface friction, packing fraction, etc.), ρ is the density of the glass beads, and g is gravitational acceleration. We verified this expected dependence of F on d_c and H as shown in Fig. 6. The power spectra as
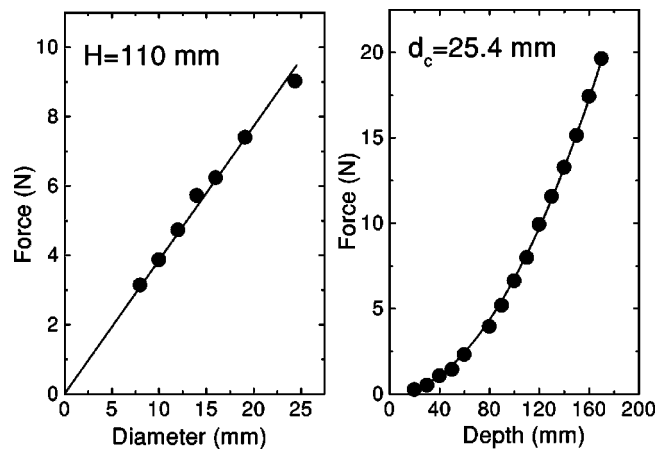

FIG. 6. The mean value of the drag force as a function of diameter and depth. The force has a quadratic dependence on the depth and a linear dependence on the diameter of the cylinder ($d_g=0.9$ mm).
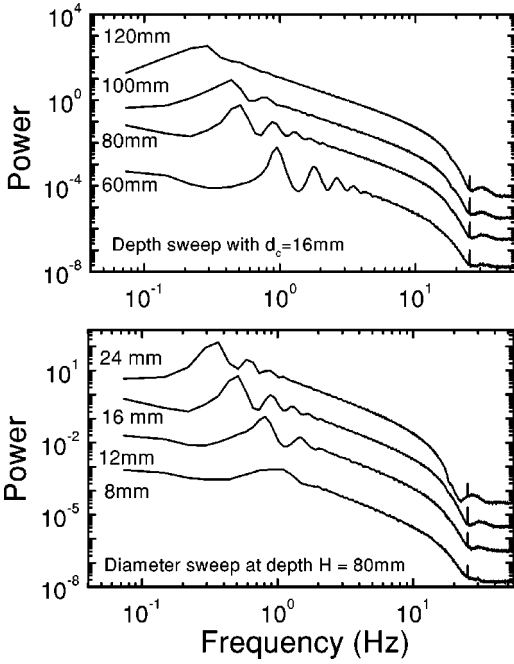
FIG. 7. Power spectra for different depths with cylinder diameter $d_c = 16$ mm (upper graph) and different diameters at depth $H = 80$ mm (lower graph), both for $d_g = 0.9$ mm. Data are vertically offset for clarity.

functions of both depth and cylinder diameter are also presented in Fig. 7.

When we varied the grain diameter d_g our results were always in agreement with our general formula: $\overline{F} = \eta \rho g d_c H^2$. In this formula η describes only the surface properties of the granular material; therefore, the average force is expected to be independent of the grain size d_g. As we show in Fig. 8. while there is some scattering around the mean for the experimentally measured values of η there is no trend corresponding to the change in grain diameter. The period, the time interval between two peaks, is connected to the change in the force via the formula $T = \Delta F / k v$ and also shows a linear dependence on cylinder size (Fig. 9) and a quadratic dependence on depth up to $H = 80$ mm.
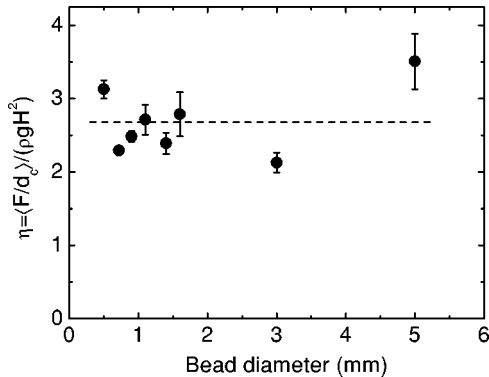

FIG. 8. The drag coefficient $\eta = \langle F/d_c \rangle / (\rho g H^2)$ as a function of bead diameter. These data are for $H = 80$, and for each data point we averaged over five cylinder diameters. The error bars represent the standard deviation.
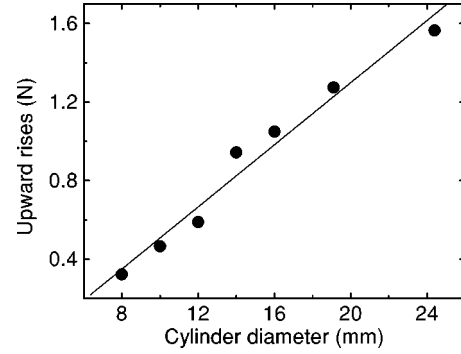

FIG. 9. Dependence of the size of upward rises (minima to next maxima) in the force on the cylinder diameter ($d_g = 0.9$ mm, $H = 80$ mm).

3. Scaling with k and v

Since our apparatus allowed us to vary k and v, we first verified whether the overall behavior of the medium is influenced by the choice of these parameters. From a methodological standpoint, decreasing speed or decreasing k affect the results in a similar way, by reducing the number of stick-slip events within a certain time interval and thus increasing the time resolution of all such events. We were able to vary k between 5 N/cm and 800 N/cm, and we found that above $k = 100$ N/cm the signal started to lose its shape and became more and more distorted with increasing k (see Fig. 10).

Since the amplitude of the signal and thus the period are inversely proportional to k, increasing k reduced the duration of the process during which the cylinder moved with the medium (t_{stick}) to the point at which the inertial effects and the elasticity of the jammed medium and apparatus were interfering with the force measurements. This set an upper
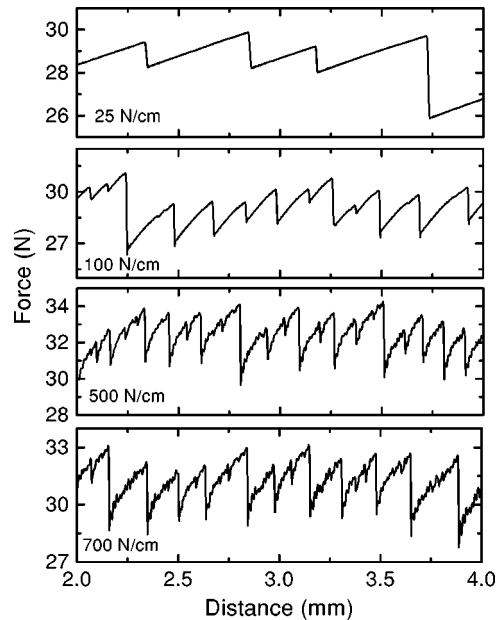

FIG. 10. The effect of increasing k on the signal. At very high spring stiffness the nonuniform elasticity of the apparatus will dominate the response and the inertial effects play an increasing role ($H = 170$ mm, $d_c = 10$ mm, $d_g = 0.9$ mm).
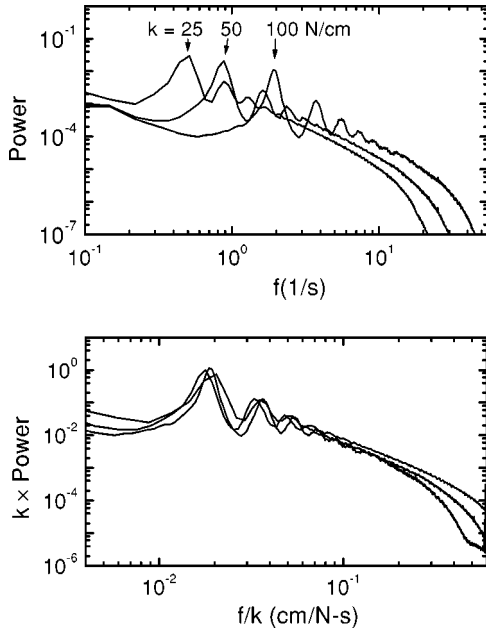
FIG. 11. Scaling with k in the periodic regime. The spring constant was varied from 25 to 100 N/cm with the leftmost peak corresponding to the weakest spring ($H=80$ mm, $d_c=16$ mm, $d_g=0.9$ mm).

limit for acceptable values of k. Below this limit, however, we could not observe any influence of k on the data. We verified this assumption by rescaling the spectra corresponding to the formula $\Delta F = kv\Delta t$. If k and v affect the data only via this relation then the scaled power spectra expressed as $kvP(\omega)=f(\omega/kv)$ should overlap.

As seen in Fig. 11, the power spectra collapse very well with k (for data taken with constant v). A similar scaling performed for the speed v, with v varied from 0.05 mm/s to 0.5 mm/s, is shown in Fig. 12 (k fixed). Based on these two results we believe that the choices of k and v did not affect the nature of the force fluctuations measured by this experiment, i.e., that the force fluctuations represent static properties of the grains rather than the measurement process.

4. Surface friction and cylinder profile

We varied the friction coefficient of the surface of the cylinders by using cylinders made from different materials. We tested sand-blasted aluminum and steel, smooth Plexiglass, and Teflon coated steel cylinders. By this substitution we varied the static friction coefficient by a factor of ≈ 2.5 [19]. The mean drag force was almost identical for all of these cylinders (within 5%) and the fluctuations also showed no qualitative difference (Fig. 13).

Thus, it appears that the frictional forces at the surface of an object have a negligible contribution to the drag force. This implies that the fluctuations originate in the bulk of the medium. It is also noteworthy that the mass of these cylinders varied significantly (the steel was around three times heavier than the aluminum cylinder) demonstrating that inertial effects are not significant.

We have also tested the effects of the shape of the object on the drag force, and we found similarly unexpected behav-
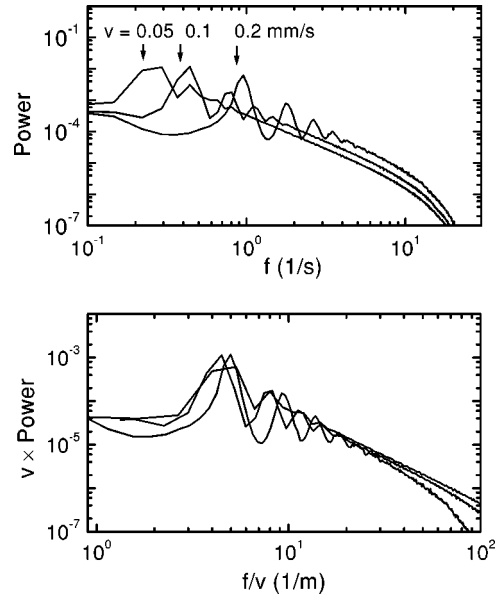

FIG. 12. Scaling with v in the periodic regime. The speed was varied from 0.05 to 0.2 mm/s with the leftmost peak corresponding to the lowest speed ($H=60$ mm, $d_c=16$ mm, $d_g=0.9$ mm).

ior. There was very little difference in the signal profile when we substituted our circular cylinder with a half cylinder with the plane of the cut perpendicular to the direction of motion. While we do not want to suggest that the force is totally independent of the shape of the object it is clear that the shape has a much smaller impact than one would expect from an analogy with the shape effects on the drag in fluids (Fig. 14). For a more detailed study, see Ref. [23].

This relative independence of cylinder shape and surface properties can, however, be explained qualitatively as a consequence of the nature of force propagation in granular media. As the cylinder advances it has to displace material through dilation; thus it has to reorganize the grains into spatially different positions. Since the force chains have a long-range character, the volume of the material resisting the movement is much larger than the volume of material engaged in frictional interactions at the surface of the object. The intergrain interactions are not only independent of the cylinder-grain interactions but they are also far more numer-
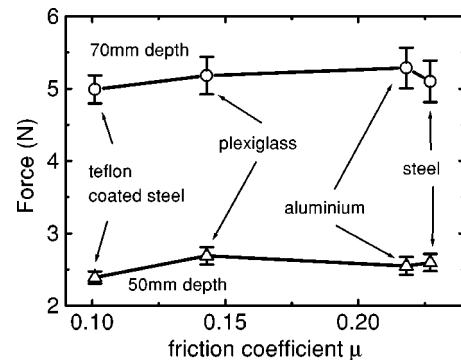

FIG. 13. Effects of the surface friction of the cylinder on the mean force and fluctuations ($d_c=16$ mm, $d_g=0.9$ mm). The error bars represent the standard deviations.
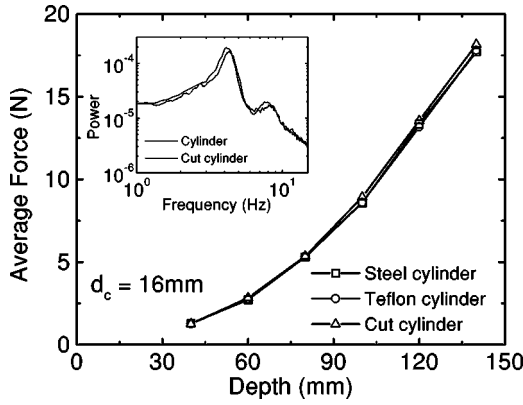
FIG. 14. Comparison of the depth dependence of the average force for different surface friction and shape ($d_g = 0.9$ mm).

ous. Thus, it is easy to see that they may completely dominate the dynamics. One can also describe this mechanism based on the energetics of the stick-slip process. The energy stored in the spring will be dissipated in friction at the surface of the object and in friction among grains far from the cylinder, as the work necessary to bring them into their new spatial positions. The number of the grains involved is not affected by the friction coefficient of the object and is only slightly influenced by the shape of the object.

B. Stepped regime

A striking feature of the data is that the fluctuations change character with depth. For smaller grains $d_g < 1.6$ mm and $H < H_c \approx 80$ mm the fluctuations are quite periodic, i.e., $F(t)$ increases continuously to a nearly constant value of F_{max} and then collapses with a nearly constant drop of ΔF (Fig. 15) as discussed above. As the depth increases, however, we observe a change in $F(t)$ to a "stepped" signal: instead of a long linear increase followed by a roughly equal sudden drop, $F(t)$ rises in small linear increments to increasing values of F_{max}, followed by small drops (in which ΔF is significantly smaller than in the rises), until F_{max} reaches a characteristic high value, at which point a large drop is observed. This transition from a periodic to a
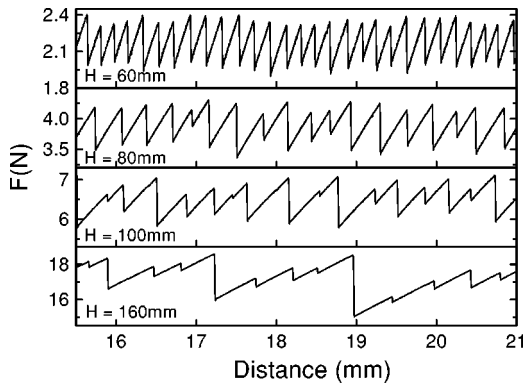

FIG. 15. The characteristic fluctuations in the drag force at four different values of H for $d_c = 10$ mm. Note the transition from purely periodic fluctuations ($H \leq 60$) to stepped fluctuations with increasing depth ($H \geq 100$).
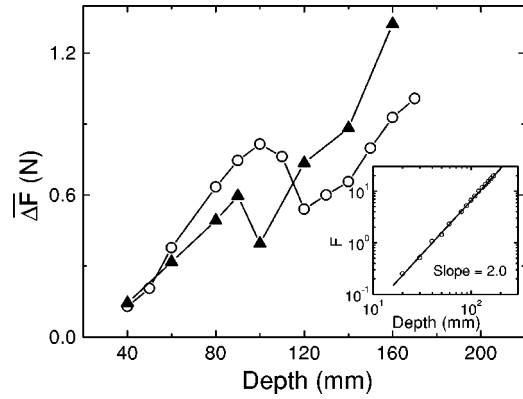

FIG. 16. The transition from periodic to stepped fluctuations as shown through the magnitude of the average drop $\overline{\Delta F}$, for two different container sizes: circles, large container ($D = 25$ mm); triangles, small container ($D = 10$ mm). The transition occurs at smaller H_c in the smaller container ($d_c = 10$ mm). The inset shows the depth dependence of the average drag force for $d_g = 1.1$ mm and $d_c = 10$ mm, and there is no change in slope at H_c. The solid line has slope 2.

stepped regime is best quantified in Fig. 16, where we plot the depth dependence of the mean of ΔF. In the periodic regime, $\overline{\Delta F}$ increases with depth just as $\overline{F}$ does. As the large uniform rises of the periodic regime are broken up by the small intermediate drops, however, $\overline{\Delta F}$ shows a local minimum and then increases continuously again. The transition can also be observed in the power spectra as shown in Fig. 7. For small depths the power spectra display a distinct peak characteristic of periodic fluctuations, but these peaks are suppressed for $H > H_c$ in correlation with the changes in the qualitative character of $F(t)$.

The transition can also be observed in the histograms (curves that can be well approximated as Gaussians) depicting the distribution of maxima and minima (Fig. 17). The initially well-separated peaks corresponding to an ideal sawtooth pattern widen while the distance between their maxima decreases up to the point at which they intersect within less than 1σ separation.

Another useful way of characterizing the structure of the fluctuations and the transition to the stepped regime is by building return maps, plotting F_N^{max} vs F_{N+1}^{max} (Fig. 18). In these plots, the continuous line shows the $F_N^{max} = F_{N+1}^{max}$ line, points above it mean that the $(N+1)$th maximum is larger than the Nth one, while points below mean that the Nth maximum is larger than the next one.

As long as there is no relation between consecutive maxima and minima these maps should not show any characteristic shape and should form a circular pattern with Gaussian spread. Indeed, at small depths we do observe such a pattern but with a somewhat elongated structure, the elongation being probably caused by the previously mentioned overall modulation of the signal. At large depths, however, the blob starts to show a structure associated with the stepped character of the motion, suggesting a history dependence in the way each jammed state will further evolve.
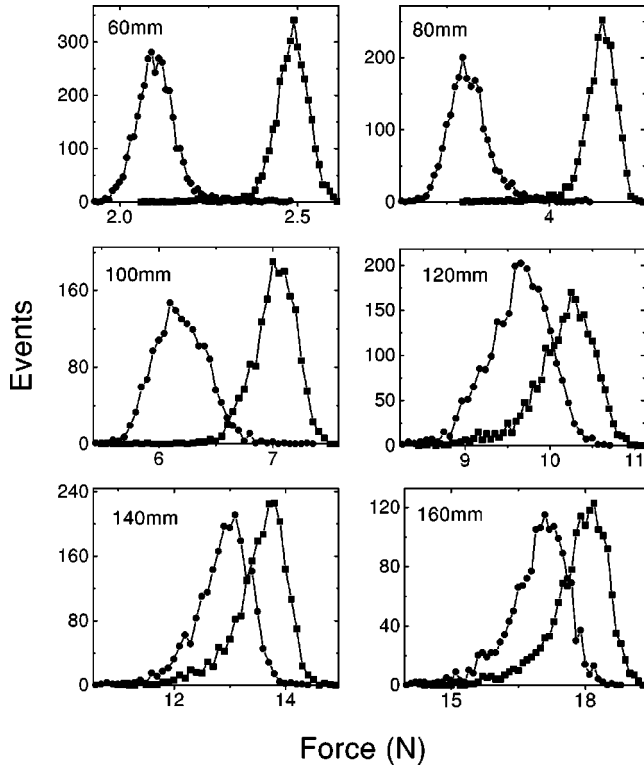
FIG. 17. Histograms of force maxima and minima for different depths. The periodic regime shows well-separated peaks while the distributions in the stepped regime overlap within one standard deviation.

The graphs show that at large depths the majority of the peaks are followed by a peak with an even greater height, and the increase from one peak to the next one is within an interval that has a well-defined upper limit. Interestingly, this limit forms a line shifted above and parallel with the line of $F_N^{max} = F_{N+1}^{max}$. Only at the highest values of F_{max} do we observe values that are smaller, usually significantly smaller

than their predecessor. This means that the force always has to first build up to a certain value before a large reorganization can occur.

C. The transition from periodic to stepped fluctuations

The transition from a periodic to a stepped signal is rather unexpected, since it implies qualitative changes in the failure and reorganization process as H increases and the existence of a critical depth, H_c. An explanation for H_c could be provided by Janssen's law [20], which states that the average pressure (which correlates directly with the local failure process) should become depth independent below some critical depth in containers with finite width. This should not occur in our container, however, which has a diameter of 25 cm, significantly larger than H_c ($\simeq 10$ cm). Furthermore, we see no deviation in the behavior of $\overline{F}(H)$ from $\overline{F} \propto H^2$, which depends on the pressure increasing linearly with the depth (Fig. 16 inset).

In order to account for the observed transition, we must inspect how the force chains originating at the surface of the cylinder nucleate the reorganizations. The motion of the cylinder attempting to advance relative to the grains is opposed by force chains that start at the cylinder's surface and propagate on average in the direction of the cylinder's motion. These force chains will terminate rather differently depending on the depth at which they originate, as shown schematically in Fig. 19. For small H, some force chains will terminate on the top surface of the granular sample and the stress can be relieved by a slight distortion of the surface. Force chains originating at large depths, however, will all terminate at the container's walls. Since the wall does not permit stress relaxation, the grains in these force chains will be more rigidly held in place. According to this picture, H_c corresponds to the smallest depth for which all force chains terminate on the wall. When the cylinder applies stress on the medium, the force chains originating at small H ($H<H_c$) reduce their
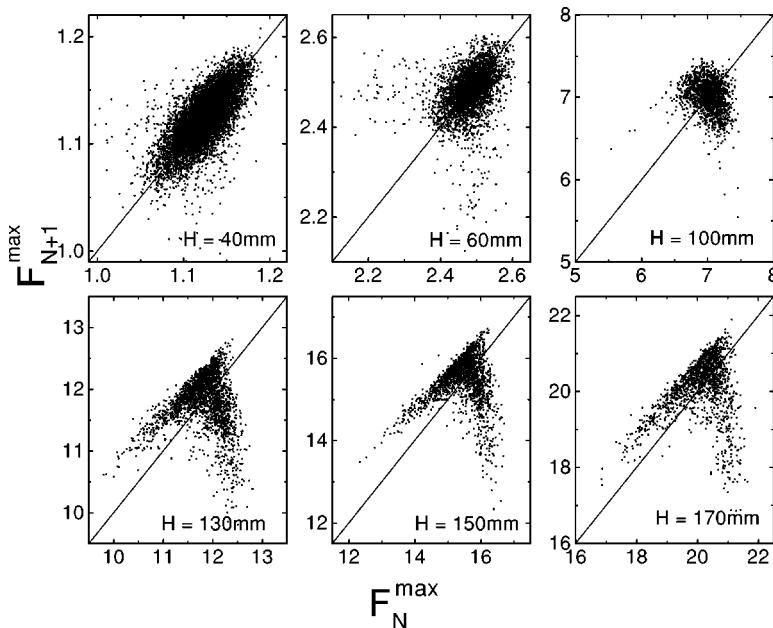

FIG. 18. The F_{N+1}^{max} vs F_N^{max} return maps for $d_g = 0.9$ mm, $d_c = 10$ mm, and different depths. The straight line is the $F_N^{max} = F_{N+1}^{max}$ line. Points above the line indicate an increasing trend of the rises; the points below show a decrease.
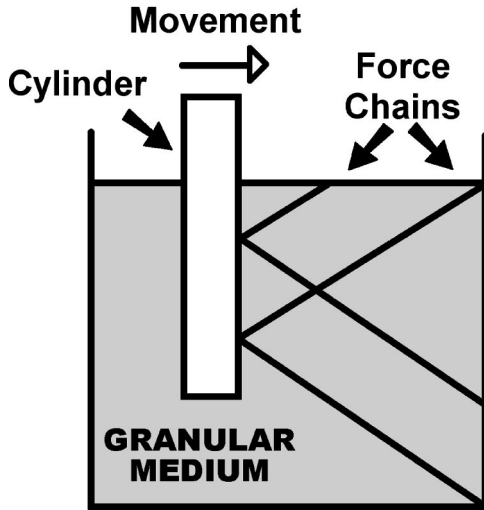
FIG. 19. Schematic diagram of the force chains perturbed by the presence of the walls. While the figure is greatly simplified since the force chains bifurcate and follow nonlinear paths, there is every reason to believe that their effective area has a conical shape.

strain through a microscopic upward relaxation of chains ending on the free surface. By contrast, the higher rigidity of force chains originating at $H > H_c$ impedes such microscopic relaxations. Thus a higher proportion of the total force applied by the cylinder will be supported by those force chains, enhancing the probability of a local slip event occurring at large depths. Such a slip event would not necessarily reorganize the grains at all depths (for example, the grains closer to the surface may not be near the threshold of reorganization);
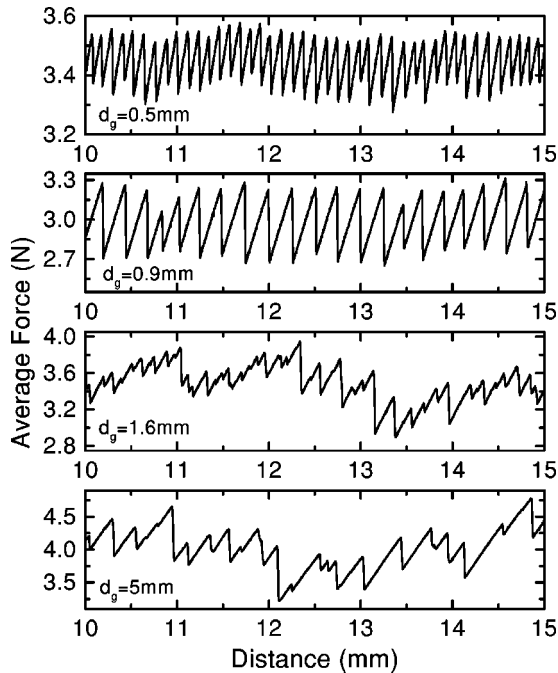

FIG. 20. Small depth ($H = 60$ mm) signal shape for different grain diameters. The small grain sizes show a well defined periodicity while the large grain sizes manifest a random pattern ($d_c = 16$ mm).
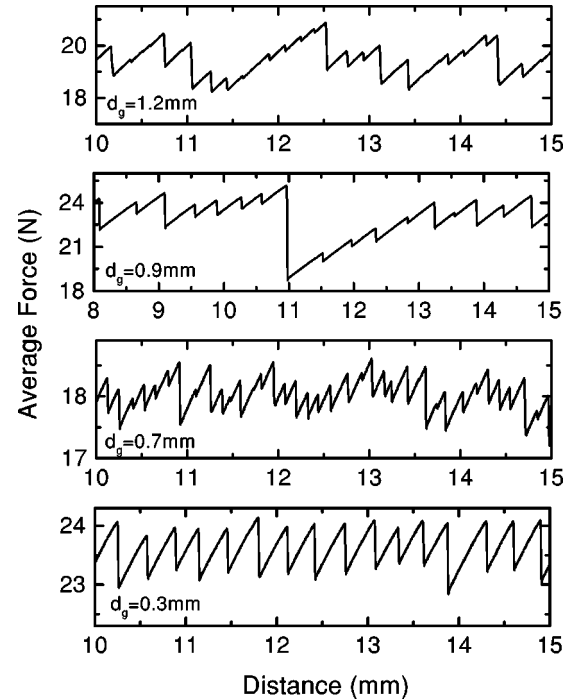

FIG. 21. Large depth signal shape for different grain diameters. The changes due to the increase in grain size cause the pattern to turn from nearly periodic to the stepped stick-slip motion with increasing grain size ($d_c = 10$ mm and $H = 140$ mm except for the 0.9 mm grains which were measured at $H = 150$ mm).

thus the slip event might induce only a local reorganization and a small drop in $F(t)$. The large drops in $F(t)$ would occur when force chains at all depths are strained to the point where the local forces are close to the threshold for a slip event. This scenario also explains why $\overline{F}(H)$ does not change at H_c, since $\overline{F}$ is determined by the collective collapse of the jammed structure of the system.

According to this picture, the transition is expected at smaller depths in smaller containers since the force chains would terminate on the walls sooner (seen Fig. 19). Indeed, as we show in Fig. 16, the transition does occur at a depth approximately 20 mm smaller when the measurements are performed in a container 2.5 times smaller (with diameter of 100 mm). Furthermore, we fail to observe the periodic fluctuations in any grains with diameters 1.4 mm or larger, which is consistent with the suggested mechanism, since larger grains correspond to a smaller effective system size [21,22].

In Fig. 20 we show how for small depths the signal changes from nearly periodic to nonperiodic just by changing the grain diameter. Similarly, the large depth regimes that show a stepped behavior become periodic for grains of smaller diameter (Fig. 21). This result is consistent with our earlier observation that reducing the container size resulted in a decrease of the H_c limit.

IV. CONCLUSIONS

In summary, we have made a detailed study of the fluctuations in granular drag. We find that the fluctuations are

strongly affected by the long-range nature of the force propagation in granular media. The jamming responsible for these fluctuations originates from a localized applied stress and our results point toward the need for a better understanding of how force chains originating from a point source propagate and disperse geometrically.

[1] For example, see, J. Geng *et al.*, Phys. Rev. Lett. **87**, 035506 (2001); G. Reydellet and E. Clement, Phys. Rev. Lett. **86**, 3308 (2001); and L. Vanel *et al.*, Phys. Rev. Lett. **84**, 1439 (2000), and references therein.

[2] M.E. Cates, J.P. Wittmer, J.-P. Bouchaud, and P. Claudin, Phys. Rev. Lett. **81**, 1841 (1998); M.E. Cates and J.P. Wittmer, Physica A **263**, 354 (1999); A.J. Liu and S.R. Nagel, Nature (London) **396**, 21 (1998).

[3] C. Liu, S.R. Nagel, D.A. Schecter, S.N. Coppersmith, S. Majumdar, O. Narayan, and T.A. Witten, Science **269**, 513 (1995); D.M. Mueth, H.M. Jaeger, and S.R. Nagel, Phys. Rev. E **57**, 3164 (1998).

[4] B. Miller, C. O'Hern, and R.P. Behringer, Phys. Rev. Lett. **77**, 3110 (1996).

[5] X. Jia, C. Caroli, and B. Velicky, Phys. Rev. Lett. **82**, 1863 (1999).

[6] E. Kolb, T. Mazozi, E. Clèment, and J. Duran, Eur. Phys. J. B **8**, 483 (1999).

[7] S.N. Coppersmith, C.-H. Liu, S. Majumdar, O. Narayan, and T.A. Witten, Phys. Rev. E **53**, 4673 (1996); M.L. Nguyen and S.N. Coppersmith, *ibid.* **59**, 5870 (1999).

[8] A.V. Tkachenko and T. Witten, Phys. Rev. E **60**, 687 (1999).

[9] L. Vanel, D. Howell, D. Clark, R.P. Behringer, and E. Clment, Phys. Rev. E **60**, 5040 (1999); D. Howell, R.P. Behringer, and C. Veje, Phys. Rev. Lett. **82**, 5241 (1999).

[10] G. Reydellet and E. Clment, Phys. Rev. Lett. **86**, 3308 (2001).

[11] I. Albert, P. Tegzes, B. Kahng, R. Albert, J.G. Sample, M. Pfeifer, A.-L. Barabási, T. Vicsek, and P. Schiffer, Phys. Rev. Lett. **84**, 5122 (2000).

[12] Sensotec, Precision Miniature Load Cell, Model 31, 10 lbs range.

[13] V. Buchholtz and T. Poschel, Granular Matter **1**, 33 (1998).

[14] O. Zik, J. Stavans, and Y. Rabin, Europhys. Lett. **17**, 315 (1992).

[15] It is an experimental observation of sliding friction that stick-slip behavior disappears if the spring k is stiff enough, or if the sliding velocity v is high enough. For an overview article, see B. N. J. Persson, Surf. Sci. Rep. **33**, 33 (1999).

[16] A.L. Demirel and S. Granick, Phys. Rev. Lett. **77**, 4330 (1996); H.J.S. Feder and J. Feder, *ibid.* **66**, 2669 (1991).

[17] R. Albert, M.A. Pfeifer, A.-L. Barabasi, and P. Schiffer, Phys. Rev. Lett. **82**, 205 (1999).

[18] S. Nasuno, A. Kudrolli, and J.P. Gollub, Phys. Rev. Lett. **79**, 949 (1997); S. Nasuno, A. Kudrolli, A. Bak, and J.P. Gollub, Phys. Rev. E **58**, 2161 (1998); J.-C. Geminard, W. Losert, and J.P. Gollub, *ibid.* **59**, 5881 (1999).

[19] We measured the friction angle φ for the cylinders sliding on a plate covered with glass beads glued onto its surface [$\mu = \tan(\varphi)$].

[20] R. L. Brown and J. C. Richards, *Principles of Powder Mechanics* (Pergamon Press, Oxford, 1970).

[21] This is why we chose to explain the periodic-stepped transition in the context of container size and not grain diameter.

[22] A. Ngadi and J. Rajchenbach, Phys. Rev. Lett. **80**, 273 (1998).

[23] I. Albert *et al.*, e-print cond-mat/0107392.